

# Evidence for a Partially Folded Intermediate in $\alpha$ -Synuclein Fibril Formation\*

Received for publication, December 4, 2000, and in revised form, January 4, 2001  
Published, JBC Papers in Press, January 10, 2001, DOI 10.1074/jbc.M010907200

Vladimir N. Uversky‡, Jie Li, and Anthony L. Fink§

From the Department of Chemistry and Biochemistry, University of California, Santa Cruz, California 95064

**Intracellular proteinaceous aggregates (Lewy bodies and Lewy neurites) of  $\alpha$ -synuclein are hallmarks of neurodegenerative diseases such as Parkinson's disease, dementia with Lewy bodies, and multiple systemic atrophy. However, the molecular mechanisms underlying  $\alpha$ -synuclein aggregation into such filamentous inclusions remain unknown. An intriguing aspect of this problem is that  $\alpha$ -synuclein is a natively unfolded protein, with little or no ordered structure under physiological conditions. This raises the question of how an essentially disordered protein is transformed into highly organized fibrils. In the search for an answer to this question, we have investigated the effects of pH and temperature on the structural properties and fibrillation kinetics of human recombinant  $\alpha$ -synuclein. Either a decrease in pH or an increase in temperature transformed  $\alpha$ -synuclein into a partially folded conformation. The presence of this intermediate is strongly correlated with the enhanced formation of  $\alpha$ -synuclein fibrils. We propose a model for the fibrillation of  $\alpha$ -synuclein in which the first step is the conformational transformation of the natively unfolded protein into the aggregation-competent partially folded intermediate.**

Sporadic Parkinson's disease is the second most common neurodegenerative disease and the most common age-related movement disorder. Parkinson's disease arises from the loss of dopaminergic neurons in the substantia nigra and is accompanied by the presence of intracellular inclusions, Lewy bodies and Lewy neurites (1). Abundant Lewy bodies and Lewy neurites in the cerebral cortex are also pathological hallmarks of dementia with Lewy bodies, a common late-life dementia that is clinically similar to Alzheimer's disease (2). Furthermore, Lewy bodies have been detected in the Lewy body variant of Alzheimer's disease (3). Structurally, Lewy bodies and Lewy neurites are composed of filamentous and granular material (4), the major component of which is  $\alpha$ -synuclein (5, 6). Two different missense mutations in the  $\alpha$ -synuclein gene, corresponding to A53T and A30P substitutions, have been identified in two kindreds with autosomal dominantly inherited, early-onset Parkinson's disease (7, 8).  $\alpha$ -Synuclein appears to be the major component of neuronal and glial inclusions in multiple system atrophy and Hallervorden-Spatz disease (9–12). Thus,

the accumulation of  $\alpha$ -synuclein-derived fibrillar material represents a critical biomedical problem.

$\alpha$ -Synuclein is a 140-amino acid protein of unknown function that was first isolated from synaptic vesicles of *Torpedo californica* and rat brain (13, 14). Purified human  $\alpha$ -synuclein has been shown to be unstructured in aqueous solution and hence extremely heat-stable (15). The amino acid sequence of  $\alpha$ -synuclein is characterized by six imperfect repeats (consensus KTKEGV) within the N-terminal half of the polypeptide as well as by a highly acidic C-terminal region (14, 17). Although the function of  $\alpha$ -synuclein is unclear, it is predominantly concentrated in the cytosol and presynaptic nerve terminals of neurons, with some fractions associated with synaptic vesicle membranes (14, 18–20). The repeat sequences in  $\alpha$ -synuclein are predicted to form amphipathic helices that can associate with lipid vesicles (18), and it has been shown to bind to small synthetic unilamellar vesicles (21), acidic and neutral phospholipid vesicles (22), and rat brain vesicles (23). It has recently been reported that  $\alpha$ -synuclein may regulate the size of presynaptic vesicular pools (24). These studies suggest that  $\alpha$ -synuclein may play a role in neurotransmission or in the organization and regulation of synaptic vesicles. The potential role of  $\alpha$ -synuclein deposition in several neurodegenerative diseases has focused attention on this protein.

The aggregation behavior of recombinant wild-type  $\alpha$ -synuclein and its A30P and A53T mutants has been studied under *in vitro* physiological conditions. It has been established that all three proteins, as well as the 1–87 and 1–120 truncated forms of recombinant  $\alpha$ -synuclein, are able to assemble readily into filaments with morphologies and staining characteristics similar to those extracted from disease-affected brain (25–27).

Unfortunately, little is currently known about the structural basis for  $\alpha$ -synuclein fibrillation. A major fundamental question concerns how the essentially disordered (“natively unfolded”) protein is transformed into the highly organized fibrils with characteristic crossed  $\beta$ -conformation. As a start to unravel the “mystery” of  $\alpha$ -synuclein fibrillation, we describe the effects of pH and temperature on the structural and fibrillation properties of human  $\alpha$ -synuclein. Since most aggregating protein systems probably involve a transient partially folded intermediate as the key precursor to fibrillation, we sought conditions that would be expected to favor such a conformation for  $\alpha$ -synuclein. The natively unfolded character of  $\alpha$ -synuclein arises from its low intrinsic hydrophobicity and high net charge at neutral pH (pI 4.7) (28). Thus, conditions that decrease the net charge and that increase the hydrophobicity would be expected to result in partial folding. Acidic pH and elevated temperatures provide such conditions, respectively. The strong correlation observed between the degree of protein folding and the efficiency of its fibril formation suggests that the intermediate can be a precursor of fibrils. Although low pH and high

\* This work was supported in part by a grant from the National Institutes of Health. The costs of publication of this article were defrayed in part by the payment of page charges. This article must therefore be hereby marked “advertisement” in accordance with 18 U.S.C. Section 1734 solely to indicate this fact.

‡ Supported by fellowships from the Parkinson's Institute and the National Parkinson's Foundation.

§ To whom correspondence should be addressed. Tel.: 831-459-2744; Fax: 831-459-2935; E-mail: enzym@cats.ucsc.edu.

temperature are unphysiological, they provide a useful model by increasing the concentration of the critical intermediate.

#### EXPERIMENTAL PROCEDURES

**Materials**—Thioflavin T (ThT)<sup>1</sup> and 1-anilinoanthracene-8-sulfonic acid (ANS) were obtained from Sigma. All other chemicals were of analytical grade and were from Fisher.

**$\alpha$ -Synuclein Expression and Purification**—A new procedure for producing and purifying  $\alpha$ -synuclein was developed by fusing its gene to a chitin-binding domain/intein system (IMPACT, New England Biolabs Inc.) and expressing the fusion protein in *Escherichia coli*. This system allowed simple purification of  $\alpha$ -synuclein by binding of the chitin-binding domain fusion protein to a chitin column, followed by addition of a thiol agent (dithiothreitol or cysteine) to induce the cleavage reaction of the intein and to release the  $\alpha$ -synuclein. The resultant protein, which was highly homogeneous upon polyacrylamide gel electrophoresis, was indistinguishable from authentic  $\alpha$ -synuclein based on its electrophoretic mobility and molecular mass determined by electrospray mass spectrometry.

**Fibril Formation**—Solutions of 0.5 ml of  $\alpha$ -synuclein at pH 7.5 in 20 mM Tris buffer or at pH 3.0 in 20 mM acetate buffer were stirred at 37 °C in glass vials with micro-stir bars. Protein concentration was 0.5 mg/ml. Fibril formation was monitored with thioflavin T fluorescence (29, 30). Aliquots of 10  $\mu$ l were removed from the incubated sample and added to 1.0 ml of 25  $\mu$ M ThT in 50 mM Tris buffer (pH 8.0) (see below). The presence of fibrils was confirmed by electron microscopy (negative staining with uranyl acetate) and atomic force microscopy.

**Analysis of Fibrillation Kinetics**—The kinetics of  $\alpha$ -synuclein fibril formation could be described as sigmoidal curves defined by an initial lag phase, in which a negligible change in ThT fluorescence intensity was observed; a subsequent exponential growth phase, in which ThT fluorescence increased; and a final equilibrium phase, in which ThT fluorescence reached a plateau, indicating the end of fibril formation. ThT fluorescence measurements were plotted as a function of time and fitted to a curve described by Equation 1,

$$Y = (y_i + m_x) + \frac{(y_f + m_x)}{1 + e^{-\frac{x-x_0}{\tau}}} \quad (\text{Eq. 1})$$

where  $Y$  is the fluorescence intensity and  $x_0$  is the time to 50% of maximal fluorescence. The initial base line during the lag phase is described by  $y_i + m_x$ . The final base line after the growth phase had ended is described by  $y_f + m_x$ . The apparent first-order rate constant ( $k_{\text{app}}$ ) for the growth of fibrils is calculated as  $1/\tau$ , and the lag time is calculated as  $x_0 - 2\tau$ . This expression is unrelated to the underlying molecular events, but provides a convenient method for comparison of the kinetics of fibrillation.

**Circular Dichroism Measurements**—CD spectra were obtained with an Aviv 60DS spectrophotometer using an  $\alpha$ -synuclein concentration of 0.5 mg/ml. Spectra were recorded in a 0.01-cm cell from 250 to 190 nm with a step size of 0.5 nm, a bandwidth of 1.5 nm, and an averaging time of 10 s. For all spectra, an average of five scans was obtained. CD spectra of the appropriate buffers were recorded and subtracted from the protein spectra.

**Fluorescence Measurements**—Fluorescence measurements were performed in semimicro-quartz cuvettes (Hellma) with a 1-cm excitation light path using a FluoroMax-2 spectrofluorometer (Instruments S. A., Inc.). ThT fluorescence was recorded immediately after addition of the aliquots to the ThT mixture from 470 to 560 nm with excitation at 450 nm, an increment of 1 nm, an integration time of 1 s, and slits of 5 nm for both excitation and emission. For each sample, the signal was obtained as the ThT intensity at 482 nm from which was subtracted a blank measurement recorded prior to addition of  $\alpha$ -synuclein to the ThT solution. ANS emission spectra were recorded from 460 to 600 nm with excitation at 350 nm, an increment of 1 nm, an integration time of 1 s, and slits of 5 nm for both excitation and emission. All data were processed using DataMax/GRAMS software.

**FTIR Spectra**—Attenuated total reflectance data were collected on a Nicolet 800SX FTIR spectrometer equipped with an MCT detector. The internal reflectance element (72  $\times$  10  $\times$  6 mm, 45° germanium trapezoid) was held in a modified SPECAC out-of-compartment attenuated total reflectance apparatus. The hydrated thin films were prepared as

described previously (31, 32). Typically, 1024 interferograms were co-added at 4-cm<sup>-1</sup> resolution. Data analysis was performed with GRAMS32 (Galactic Industries Corp.). Secondary structure content was determined from curve fitting to spectra deconvoluted using second derivatives and Fourier self-deconvolution to identify component band positions. Hydrated thin film samples were prepared by drying 50  $\mu$ l of 1 mg/ml  $\alpha$ -synuclein solution on a ZnSe crystal with dry N<sub>2</sub>. The IR spectra were collected, followed by Fourier transformation using the spectrum of the clean crystal as a background. Water (liquid and vapor) components were subtracted from the protein spectrum.

**Small Angle X-ray Scattering Experiments**—Small angle x-ray scattering (SAXS) measurements were made using Beam Line 4-2 at the Stanford Synchrotron Radiation Laboratory (33). X-ray energy was selected at 8980 eV (copper edge) by a pair of Mo/B<sub>4</sub>C multilayer monochromator crystals (34). Scattering patterns were recorded by a linear position-sensitive proportional counter, which was filled with an 80% xenon and 20% CO<sub>2</sub> gas mixture. Scattering patterns were normalized by incident x-ray fluctuations, which were measured with a short length ion chamber before the sample. The sample-to-detector distance was calibrated to be 230 cm using a cholesterol myristate sample. The measurements were performed in a 1.3-mm path length observation static cell with 25- $\mu$ m mica windows. To avoid radiation damage of the sample in SAXS measurements, the protein solution was continuously passed through a 1.3-mm path length observation flow cell with 25- $\mu$ m mica windows. Background measurements were performed before and after each protein measurement and then averaged before being used for background subtraction. All SAXS measurements were performed at 23  $\pm$  1 °C.

The radius of gyration ( $R_g$ ) was calculated according to the Guinier approximation (35),  $\ln I(Q) = \ln I(0) - R_g^2 Q^2/3$ , where  $Q$  is the scattering vector given by  $Q = (4\pi \sin \theta)/\lambda$ , where  $2\theta$  is the scattering angle and  $\lambda$  is the wavelength of x-ray.  $I(0)$ , the forward scattering amplitude, is proportional to  $n \rho_c^2 V^2$ , where  $n$  is the number of scatterers (protein molecules) in solution,  $\rho_c$  is the electron density difference between the scatterer and the solvent, and  $V$  is the volume of the scatter. This means that the value of forward scattered intensity,  $I(0)$ , is proportional to the square of the molecular mass of the molecule (35). Thus,  $I(0)$  for a pure  $n$ -mer sample will therefore be  $n$ -fold that for a sample with the same number of monomers since each  $n$ -mer will scatter  $n^2$  times as strongly as monomer; but in this case, the number of scattered particles ( $n$ -mers) will be  $n$  times less than that in the pure monomer sample.

#### RESULTS AND DISCUSSION

On the one hand, as noted,  $\alpha$ -synuclein belongs to the class of natively unfolded proteins, which have little or no ordered structure in the purified state under physiological conditions (15); and on the other, it forms fibrils of highly organized secondary structure. For example, x-ray diffraction analysis of  $\alpha$ -synuclein fibrils shows the characteristic pattern of a crossed  $\beta$ -sheet structure, in which the  $\beta$ -strands lie perpendicular to the long fiber axis, typical of all amyloid fibrils (27). Electron microscopy analysis indicates that human  $\alpha$ -synuclein filaments are typically 6–9 nm in width and several microns long (27). Clearly, within the fibril,  $\alpha$ -synuclein cannot be present as an extended linear polymer since, in a fully extended conformation, the maximal linear dimension of a polypeptide with  $n$  residues is  $n \times 3.63$  Å (36). This gives  $\sim$ 51 nm for  $\alpha$ -synuclein, which is at least five times greater than the diameter of the filament.

A fundamental question is what forces or factors will cause a natively unfolded protein to fold. It has been shown that natively unfolded proteins are characterized by a unique combination of low overall hydrophobicity and large net charge (28). Based on this observation, it is reasonable to suggest that any alterations in the protein environment leading to an increase in its hydrophobicity and/or a decrease in its net charge should be accompanied by at least partial folding of the intrinsically disordered protein. The overall hydrophobicity of a protein will increase with increasing temperature (the hydrophobic interaction has the unusual property of increasing in magnitude at higher temperatures due to the large change in heat capacity with temperature and the complex thermodynamic properties associated with changes in water structure as the temperature

<sup>1</sup> The abbreviations used are: ThT, thioflavin T; ANS, 1-anilinoanthracene-8-sulfonic acid; FTIR, Fourier transform infrared; SAXS, small angle x-ray scattering.

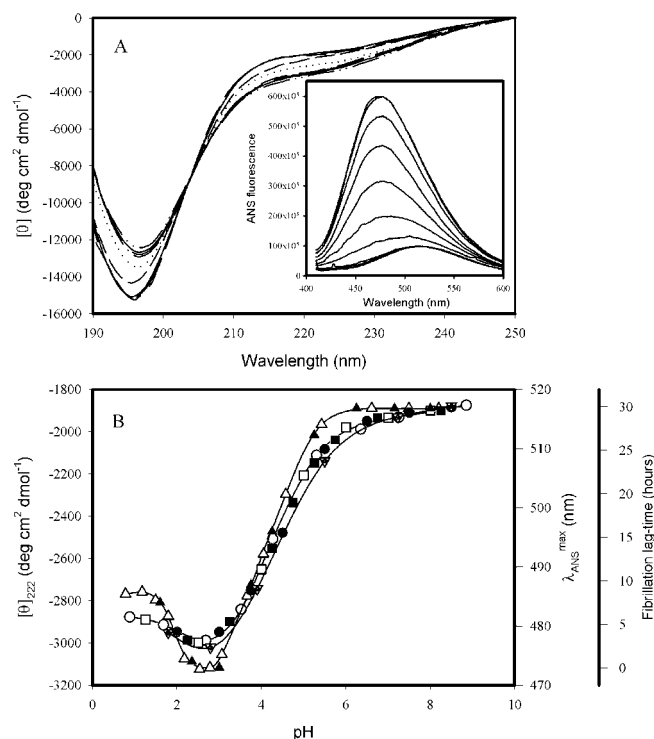


**FIG. 1. Effect of pH on the structural properties of  $\alpha$ -synuclein.** A, far-UV CD spectra as a function of pH. pH values were 8.9 (solid line), 7.3, 6.4, 5.3, 4.3, 3.5, 2.7, 1.7, and 0.9 in order of the increase in negative  $[\theta]_{222}$  value. The inset represents ANS fluorescence spectra measured at pH 8.2, 7.5, 6.6, 5.4, 4.6, 4.0, 3.7, 3.1, 2.8, and 2.5 (in order of increasing intensity). B, comparison of the effect of pH on far-UV circular dichroism (circles and squares) and ANS fluorescence (triangles) spectra. The results of the initial titration (decrease in pH) and reverse (increase in pH) experiments are presented as open and closed symbols, respectively. The cell path length was 0.1 and 10 mm for far-UV CD and fluorescence measurements, respectively. Measurements were carried out at 20 °C. Protein concentration was 0.1 (circles), 1.0 (squares), and 0.01 (triangles) mg/ml. Data on the pH effect on the lag time of  $\alpha$ -synuclein fibrillation ( $\nabla$ ) are also shown for comparison. deg, degrees.

increases) (37), and the excess negative charge of  $\alpha$ -synuclein at neutral pH (pI 4.7) would be neutralized at lower pH values. Thus, we can expect partial folding of  $\alpha$ -synuclein under conditions of high temperature and/or low pH. In contrast to an unfolded protein, a partially folded intermediate is anticipated to have contiguous hydrophobic patches on its surface, which are likely to foster self-association and hence potentially fibrillation.

The advantages of using high temperatures or lower pH are that these conditions are anticipated to dramatically increase the population of putative partially folded intermediates, thus making it easier to characterize them. Such intermediates will be in equilibrium with the natively unfolded conformation and presumably are not populated significantly under normal physiological conditions.

#### Effect of pH on $\alpha$ -Synuclein Structure and Fibrillation

**Far-UV Circular Dichroism**—Fig. 1A represents the far-UV CD spectra of human recombinant  $\alpha$ -synuclein measured at different pH values at 20 °C. At neutral pH, the protein possesses a far-UV CD spectrum typical of an essentially unfolded polypeptide chain. The spectrum has an intense minimum in the vicinity of 196 nm, with the absence of characteristic bands in the 210–230 nm region. However, as the pH was decreased, changes were observed in the shape of the spectrum. Fig. 1 shows that the minimum at 196 nm became less intense, whereas the negative intensity of the spectrum around 222 nm

increased, reflecting pH-induced formation of secondary structure. The pH dependence of  $[\theta]_{222}$  is shown in Fig. 1B. There was little change in the far-UV CD spectrum between pH  $\sim$ 9.0 and  $\sim$ 5.5. However, a decrease in pH from 5.5 to 3.0 resulted in a  $\sim$ 2-fold increase in negative intensity in the vicinity of 220 nm, and a further decrease in pH was accompanied by a reversal in the spectral intensity. Fig. 1B shows that the pH-induced changes in the far-UV CD spectrum of  $\alpha$ -synuclein were completely reversible (compare open and closed symbols) and were independent of protein concentration (at least in the range of 0.1–1.5 mg/ml) (compare circles and squares). These observations are consistent with the assumption that the pH-induced increase in the structure of  $\alpha$ -synuclein represents an intramolecular process and not self-association. Based on additional structural probes, described below, we interpret these far-UV CD changes to reflect the formation of a partially folded intermediate with significant  $\beta$ -structure. The fact that the far-UV CD spectra of  $\alpha$ -synuclein as a function of pH show an isosbestic point (Fig. 1A) indicates that the transition is a two-state one, presumably between the natively unfolded state and the partially folded intermediate conformation.

The question arises as to whether these spectral changes correspond to a small fraction of the total protein being in the intermediate conformation, in which case the intermediate has a large negative ellipticity in the vicinity of 220 nm, or whether essentially all the molecules are present as the intermediate, in which case it has a small ellipticity at 220 nm. Based on the small angle x-ray scattering results (see below), we can conclude that the majority of the molecules are in the same conformation, and thus, the intermediate possesses limited secondary structure.

**ANS Fluorescence**—Changes in ANS fluorescence are frequently used to detect non-native partially folded conformations of globular proteins (38–40). This is because such intermediates are characterized by the presence of solvent-exposed hydrophobic clusters to which ANS binds, resulting in a considerable increase in the ANS fluorescence intensity and in a pronounced blue shift of the fluorescence emission maximum. Fig. 1 shows that, in the case of  $\alpha$ -synuclein, a decrease in pH led to a large blue shift of the ANS fluorescence maximum (from  $\sim$ 515 to  $\sim$ 475 nm) (Fig. 1B, open triangles), reflecting the pH-induced transformation from the natively unfolded state to the partially folded compact conformation. The transition from unfolded to partially folded conformation took place between pH 5.5 and 3.0 and was completely reversible (open and closed symbols).

Fig. 1B shows that the pH-induced structural transitions observed by ANS fluorescence and CD ellipticity changed simultaneously in a rather cooperative manner. This means that protonation of  $\alpha$ -synuclein results in transformation of the natively unfolded protein into a conformation with a significant amount of ordered secondary structure and with affinity for ANS. The position of the transition indicates that protonation of one or more carboxylates was responsible for the structural change. Further investigations were devoted to the structural characterization of this conformation.

**Secondary Structure Analysis by FTIR**—FTIR represents a powerful method for the investigation of protein secondary structure. The main advantage of this approach in comparison with CD is that FTIR is much more sensitive to  $\beta$ -structure. To work with low protein concentrations, we used attenuated total reflectance FTIR and hydrated thin films of the sample (31, 32). Fig. 2 shows the FTIR (amide I region) spectra of  $\alpha$ -synuclein measured at pH 7.5 and 3.0. The spectrum of  $\alpha$ -synuclein fibrils is also presented for comparison. The FTIR spectrum of  $\alpha$ -synuclein at pH 7.5 is typical of a substantially unfolded

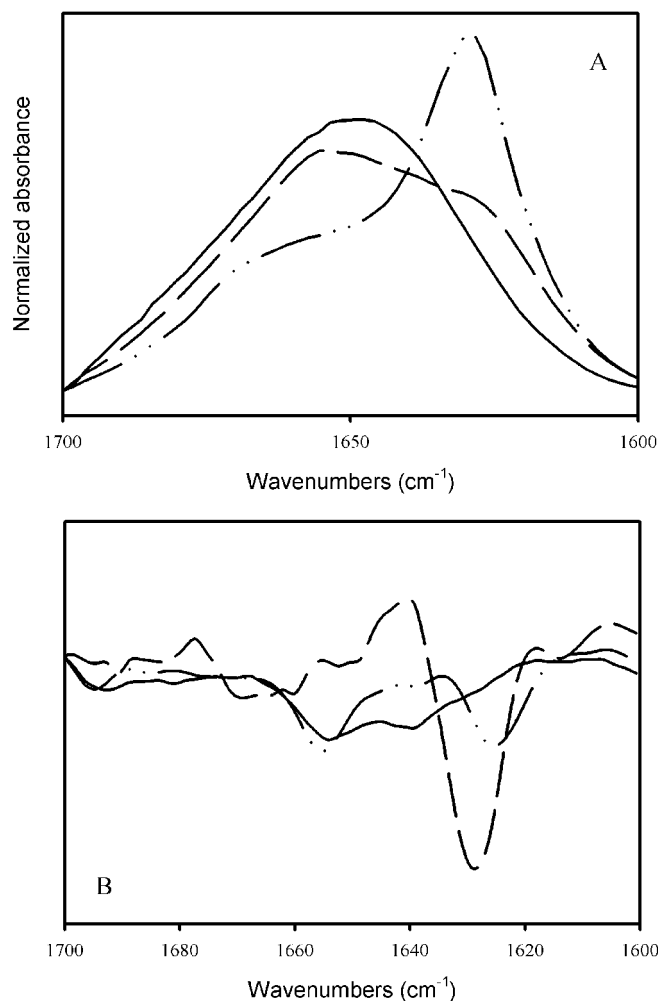


FIG. 2. Secondary structure analysis of  $\alpha$ -synuclein by FTIR. A, FTIR spectra of the amide I region were measured at pH 7.5 (solid line) and pH 3.0 (dashed line). The spectrum of  $\alpha$ -synuclein fibrils is shown for comparison (dashed and dotted line). B, shown are second derivatives of the corresponding spectra. The major  $\beta$ -structure bands are in the 1620–1640  $\text{cm}^{-1}$  region.

polypeptide chain, whereas a decrease in pH led to significant spectral changes, indicative of increased ordered structure. The most evident change was the appearance of a new band in the vicinity of 1626  $\text{cm}^{-1}$ , which corresponds to  $\beta$ -sheet. This means that, at acidic pH, natively unfolded  $\alpha$ -synuclein is transformed into a partially folded conformation with a significant amount of  $\beta$ -structure. As expected, the FTIR spectrum of  $\alpha$ -synuclein fibrils shows the major contribution from  $\beta$ -sheet. Fourier self-deconvolution (and second derivative) of the FTIR spectra followed by curve fitting revealed the differences in the secondary structure in the different conformations. These results are summarized in Table I. Based on the SAXS experiments (below), the protein is monomeric at pH 3, and thus, the increased  $\beta$ -structure is not due to association-induced  $\beta$ -sheet.

**Small Angle x-ray Scattering Studies**—SAXS is a very useful method for the investigation of conformation, shape, and dimensions of biopolymers in solution. Analysis of the scattering curves using the Guinier approximation gives information about  $R_g$ . Presentation of the scattering data in the form of Kratky plots provides information about the globularity (packing density) and conformation of a protein (35). For a native globular protein, this plot has a characteristic maximum, whereas unfolded and partially folded polypeptides have significantly different-shaped Kratky plots.

Guinier analysis of scattering data shows that, at neutral

pH,  $\alpha$ -synuclein is characterized by an  $R_g$  of  $40 \pm 1 \text{ \AA}$  (Fig. 3A). At low pH, this parameter decreases to  $30 \pm 1 \text{ \AA}$  at pH 3.0, reflecting considerable compaction of the protein, corresponding to a volume decrease of 2.4-fold. The linear Guinier plots indicate that the solutions are homogeneous, suggesting that, at pH 3, essentially all the molecules of  $\alpha$ -synuclein have the intermediate conformation, rather than a small fraction. It is interesting to compare measured  $R_g$  values with those calculated for the fully globular and random-coil polypeptide chains of 140 amino acid residues. The  $R_g$  for a native globular protein composed of  $n$  amino acid residues is given by  $R_g^N = 2.9 \cdot n^{1/3}$  (41). Thus, if  $\alpha$ -synuclein were folded into a globular structure, it would have  $R_g^N = 2.9 \cdot 140^{1/3} = 15.1 \text{ \AA}$ . The radius of gyration of a completely unfolded (random-coil) polypeptide,  $R_g^U$ , may be estimated from the corresponding Stokes radius,  $R_S^U$ , using the known relation  $R_g^U/R_S^U = 1.51$  (42). The hydrodynamic radius of a completely unfolded globular protein,  $R_S^U$ , with known molecular mass may be calculated from the following empirical equation (43):  $\log(R_S^U) = 0.533 \cdot (M) - 0.682$ . This gives 34.3  $\text{\AA}$  for  $R_S^U$  and 52.1  $\text{\AA}$  for  $R_g^U$ . The observed  $R_g$  for  $\alpha$ -synuclein at neutral pH is smaller (40  $\text{\AA}$ ) than that estimated for a random-coil conformation (52  $\text{\AA}$ ), indicating that the molecule is more compact than a random coil. On the other hand, the  $R_g$  for the partially folded intermediate (30  $\text{\AA}$ ) is much larger than that of a folded globular protein of the size of  $\alpha$ -synuclein (15  $\text{\AA}$ ).

Analysis of the x-ray scattering in the form of a Kratky plot shows that  $\alpha$ -synuclein lacks a well developed globular structure at both pH 7.5 and 3.0 (Fig. 3B). The profile of the Kratky plot at neutral pH is typical for a random-coil conformation, whereas that at pH 3 shows changes consistent with the development of the beginnings of a tightly packed core.

The SAXS forward scattering intensity values give information on the degree of protein association. The results of this analysis for  $\alpha$ -synuclein indicate that the decrease in pH was not accompanied by a significant change in this parameter:  $I(0)$  was  $0.0124 \pm 0.0004$  at pH 7.5 and  $0.0119 \pm 0.0003$  at pH 3.0. This directly confirms that the pH-induced folding of  $\alpha$ -synuclein is an intramolecular process and does not result from self-association.

**Effect of pH on  $\alpha$ -Synuclein Fibrillation**—The histological dye thioflavin T is widely used for the detection of amyloid fibrils (29, 44, 45). In the presence of fibrils, ThT gives rise to a new excitation maximum at 450 nm and enhanced emission at 482 nm, whereas unbound ThT is essentially non-fluorescent at these wavelengths. ThT is believed to interact specifically and rapidly with the crossed  $\beta$ -sheet structure common to amyloid fibrils, and the binding is independent of the primary structure of the protein. Only the multimeric fibrillar forms, not multiple  $\beta$ -sheet domains in native proteins, give significant fluorescence with ThT. The binding of ThT to  $\alpha$ -synuclein fibrils is thus a very convenient method for studying the kinetics of fibril formation.

Fig. 4 represents time-dependent changes in the ThT fluorescence during the process of  $\alpha$ -synuclein fibril formation at 37  $^\circ\text{C}$  as a function of pH. The kinetics of the ThT fluorescence intensity at 482 nm exhibit characteristic sigmoidal curves, which have of an initial lag phase, a subsequent growth phase, and a final equilibrium phase. Such curves are consistent with a nucleation-dependent polymerization model, in which the lag corresponds to the nucleation phase, and the exponential part to fibril growth (elongation) (26, 46–51)

Fig. 4 shows that decreasing the pH resulted in a very substantial acceleration of the kinetics of  $\alpha$ -synuclein fibril-

TABLE I  
Secondary structure content of human  $\alpha$ -synuclein determined by FTIR under different experimental conditions

Structural assignment	pH 7.5		pH 3.0		Fibrils, pH 7.5	
	Wave number	%	Wave number	%	Wave number	%
Turn	1688	2.9	1687	2.6	1684	3.0
Turn	1673	18.5	1672	18.3	1666	18.5
Loops/disordered	1655	38.3	1656	23.4		
Disordered/extended	1640	24.7	1642	31.1	1648	24.0
$\beta$ -Sheet	1626	15.6	1624	24.3	1629	47.1

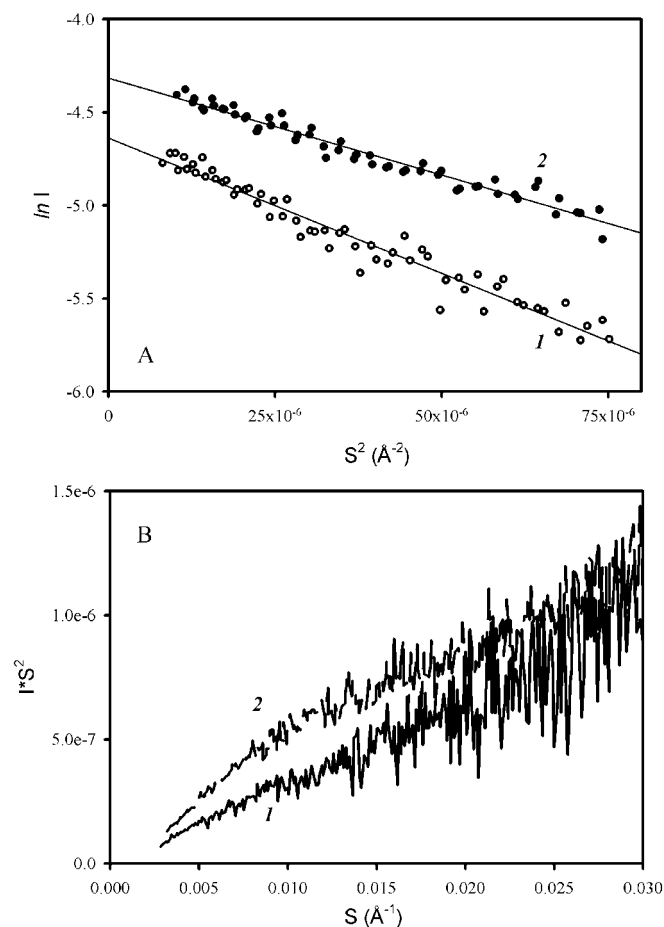


FIG. 3. Guinier (A) and Kratky (B) plot representation of the results of small angle x-ray scattering analysis of  $\alpha$ -synuclein under different experimental conditions: pH 7.5 (line 1) and pH 3.0 (line 2). Measurements were carried out at 23 °C. Protein concentration was 1.0 mg/ml.

lation: the lag time was  $\sim 12$  times shorter ( $2.4 \pm 0.06$  versus  $28.1 \pm 0.6$  h), and the apparent rate of fibril formation was  $\sim 10$ -fold larger ( $1.03 \pm 0.003$  versus  $0.11 \pm 0.007 \text{ h}^{-1}$ ) at pH 3.0 compared with pH 7.5. Fig. 4B shows that pH had similar effects on both the lag time and the elongation rate. Interestingly, the pH dependence of the kinetic parameters of fibril formation shows transitions similar to the pH dependences of the  $\alpha$ -synuclein structural parameters monitored by circular dichroism and ANS binding (cf. Figs. 1B and 4B). Moreover, Fig. 1B shows that the pH-induced changes in the  $\alpha$ -synuclein fibrillation kinetics were coincident with the pH-driven structural transformations. In other words, there was an excellent correlation between intramolecular conformational change and fibril formation. This is a very important observation and is consistent with the conclusion that the process of  $\alpha$ -synuclein fibrillation is dramatically accelerated by the partial folding of the natively unfolded protein.

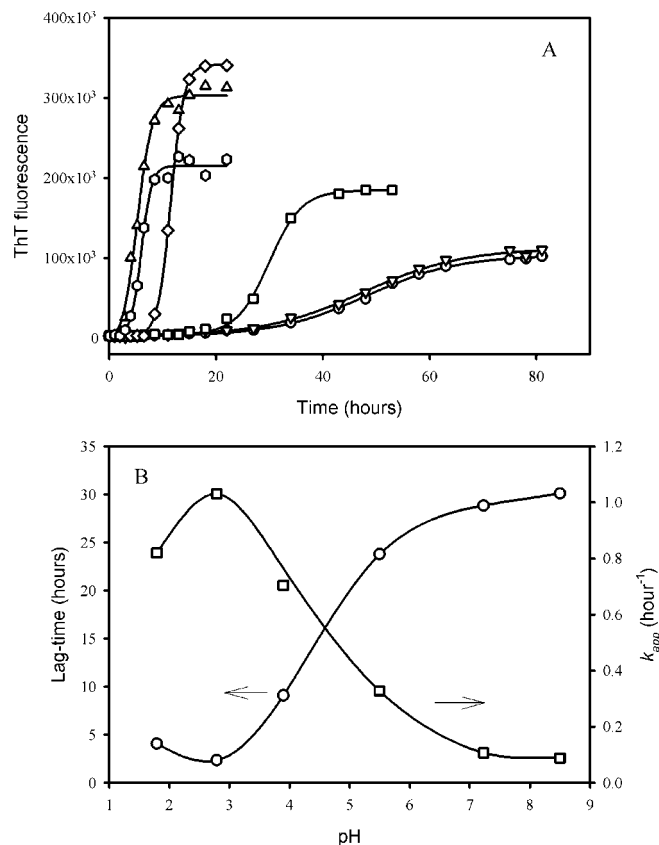


FIG. 4. Effect of pH on fibril formation of human  $\alpha$ -synuclein. A, kinetics of fibrillation monitored by the enhancement of thioflavin T fluorescence intensity. Measurements were performed at 37 °C and pH 8.52 (circles), 7.23 (inverted triangles), 5.82 (squares), 4.08 (diamonds), 2.79 (triangles), and 1.92 (hexagons). Protein concentration was 1 mg/ml. ThT fluorescence was excited at 450 nm, and the emission wavelength was 482 nm. B, pH dependence of kinetic parameters of  $\alpha$ -synuclein fibrillation: lag time (circles) and apparent rate constant of elongation (squares). The lag times at rates of elongation were determined as described under "Experimental Procedures."

#### Elevated Temperature Causes a Conformational Transition in $\alpha$ -Synuclein and Facilitates Fibrillation

Effect of Temperature on the Secondary Structure of  $\alpha$ -Synuclein—Fig. 5 represents the far-UV CD spectra of  $\alpha$ -synuclein measured at different temperatures. At low temperatures, the protein shows a far-UV spectrum typical of an unfolded polypeptide chain. As the temperature was increased, the spectrum changed, consistent with temperature-induced formation of secondary structure. The temperature dependence of  $[\theta]_{222}$  (Fig. 5, inset) shows that the major spectral changes occurred over the range of 3 to 50 °C. Further heating led to a less pronounced effect. Interestingly, Fig. 5 shows that the structural changes induced in  $\alpha$ -synuclein by heating were completely reversible (cf. open and closed circles). These data indicate that high temperatures induce a reversible transition

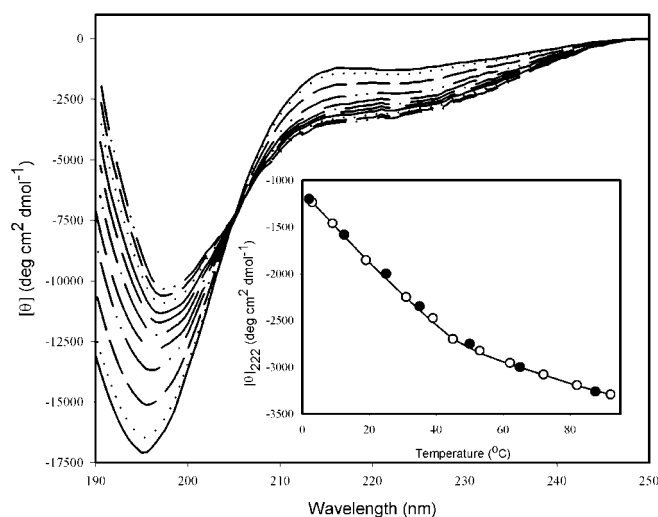


FIG. 5. **Effect of temperature on the far-UV CD spectra of  $\alpha$ -synuclein at pH 7.5.** Far-UV CD spectra were measured at increasing temperatures: 3.0, 9.0, 19.0, 31.0, 39.0, 45.0, 53.0, 62.0, 72.0, 82.0, and 92.0 °C (in order of the increase in negative  $[\theta]_{222}$  value). The inset shows the dependence of  $[\theta]_{222}$  on temperature. Data for increasing temperature and cooling are shown as open and closed circles, respectively.

in  $\alpha$ -synuclein leading to a partially folded intermediate. This intermediate has a circular dichroism spectrum similar to that induced by low pH. Since hydrophobic interactions increase with increasing temperature, the simplest explanation for the temperature-induced structural formation is that it is driven by hydrophobic interactions. The enhanced rates of fibrillation at higher temperatures probably reflect a combination of both faster rates at higher temperatures and increased concentration of the aggregation-competent intermediate due to the increased hydrophobic interactions.

**Effect of Temperature on  $\alpha$ -Synuclein Fibril Formation**—Fig. 6A shows the effect of temperature on the kinetics of  $\alpha$ -synuclein fibrillation at pH 7.5. The kinetics were strongly affected by temperature, with similar effects on both the lag time and the elongation rate. The activation energy values calculated from the slopes of corresponding Arrhenius plots (Fig. 6B) were  $17.9 \pm 0.8$  and  $20.1 \pm 0.8$  kcal/mol for the nucleation and elongation processes, respectively.

#### Fibril Morphology from Electron Microscopy

Fig. 7 shows that the fibril morphology was sensitive to the conditions under which the fibrils were formed. Fibrils formed at neutral pH and 37 °C were longer and much less clumped than those formed at higher temperature or low pH. The latter two conditions led to fibrils that were much shorter in length and of much higher fibril density. Since it has been frequently observed that fibrils made *in vitro* from a variety of proteins may have morphologies that are very sensitive to the conditions under which they were grown, we do not attach much significance to the fact that  $\alpha$ -synuclein fibril morphology varied with the choice of incubation conditions.

#### Model for Fibrillation

The data reported herein demonstrate that low pH or elevated temperature leads to formation of a partially folded intermediate conformation of  $\alpha$ -synuclein and that these conditions correlate with enhanced kinetics of fibrillation, suggesting that the intermediate is an important species on the fibril-forming pathway. The effects of low pH are attributed to minimization of the large net negative charge present at neutral pH, thereby decreasing charge-charge intramolecular re-

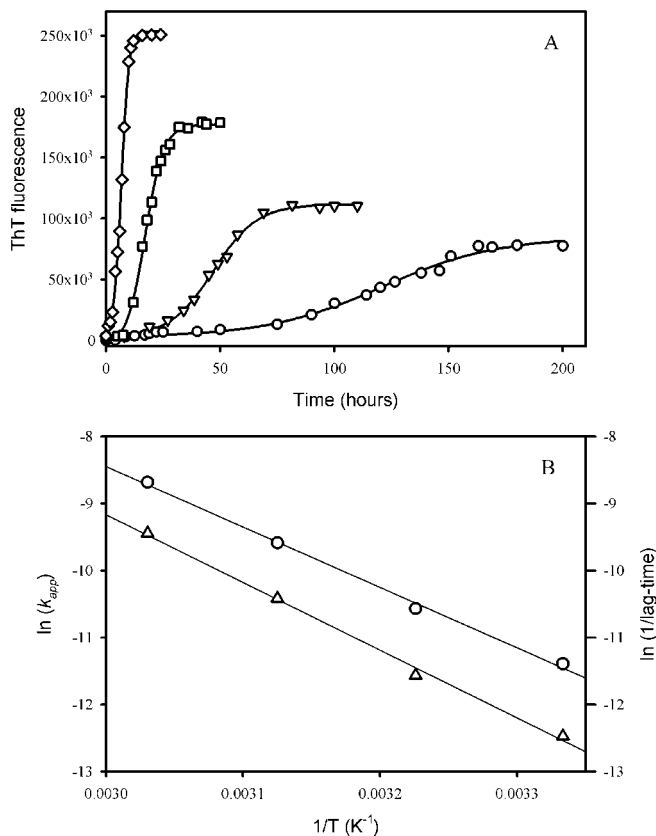


FIG. 6. **Effect of temperature on  $\alpha$ -synuclein fibrillation.** A, kinetics of fibril formation monitored by the enhancement of ThT fluorescence. Measurements were performed at 27 °C (circles), 37 °C (inverted triangles), 47 °C (squares), and 57 °C (diamonds). Protein concentration was 1 mg/ml. ThT fluorescence was excited at 450 nm, and the emission wavelength was 482 nm. The lag times at rates of elongation were determined as described under "Experimental Procedures." B, the corresponding Arrhenius plots for the lag time (circles) and the elongation rate constant (triangles).

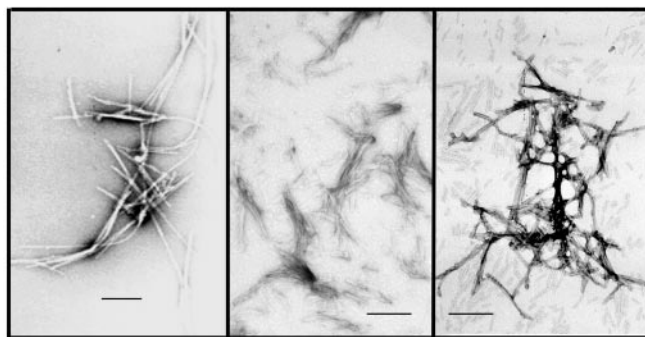


FIG. 7. **Negatively stained transmission electron micrographs of  $\alpha$ -synuclein fibrils prepared under different experimental conditions:** pH 7.5 and 37 °C (left), pH 3.0 and 37 °C (middle), and pH 7.5 and 57 °C (right). A 100-nm scale bar is shown for comparison. A magnification of 40,000 was used in all three images.

pulsion and permitting hydrophobic interaction-driven collapse to the partially folded intermediate. The effects of elevated temperatures are attributed to increased strength of the hydrophobic interaction at higher temperatures, leading to a stronger hydrophobic driving force for folding. Calculations indicate that the combination of net charge and intrinsic hydrophobicity of  $\alpha$ -synuclein is such that it is only marginally destabilized at neutral pH; thus, either relatively small increases in hydrophobicity or decreased charge is sufficient to promote its partial folding (28).

The results are consistent with the following scheme for

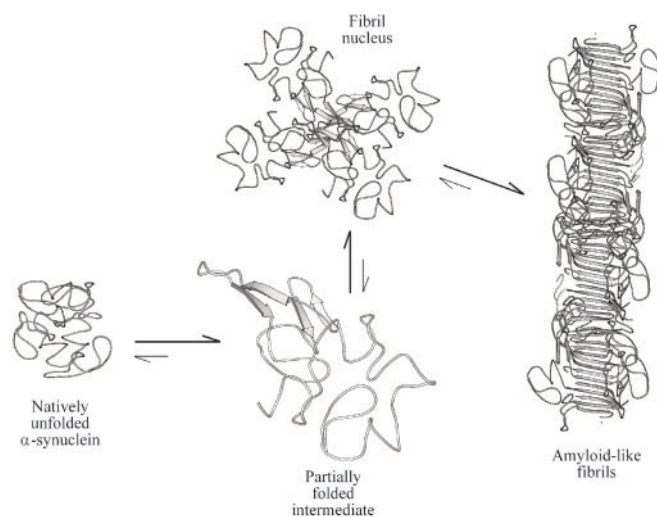


FIG. 8. **Model for  $\alpha$ -synuclein fibrillation.** Transformation of the natively unfolded protein to the partially folded intermediate leads to association due to exposed hydrophobic surfaces of the intermediate. Oligomerization of the intermediate leads either to fibrils via a critical nucleus or to soluble oligomers, resulting in amorphous aggregates. Additional conformational changes occur between the aggregation-competent intermediate and the fibrils. The oligomeric intermediate (representing the nucleus or a soluble aggregate) is shown as a tetramer for convenience only and could be much larger.

$\alpha$ -synuclein fibrillation:  $U_N \leftrightarrow I \leftrightarrow \text{Nucl} \rightarrow F$ , where  $U_N$ ,  $I$ ,  $\text{Nucl}$ , and  $F$  correspond to the natively unfolded conformation, partially folded intermediate, fibril nucleus, and fibril, respectively. From this model, we anticipate two key kinetic steps: the structural transformation leading to the intermediate, and formation of the nucleus (Fig. 8). Thus, factors that shift the equilibrium in favor of the intermediate will facilitate fibril formation, as observed. Fibril elongation could involve the addition of either the intermediate or the natively unfolded molecule to existing fibrils or seeds. Fibrillation of  $\alpha$ -synuclein, leading to Lewy body formation and Parkinson's and related Lewy body diseases, thus may arise from various factors that would significantly populate or increase the concentration of the aggregation-competent intermediate. Possibilities include nonpolar molecules (such as some pesticides) that might preferentially bind to the partially folded intermediate and cations that might mimic the effect of low pH (high proton concentration) as well as factors that result in an increase in the concentration of  $\alpha$ -synuclein itself.

There are two interesting features of the  $\alpha$ -synuclein partially folded intermediate: it has some  $\beta$ -structure, which is the major type of secondary structure in  $\alpha$ -synuclein fibrils, and it is relatively unfolded (*i.e.* more similar to a random-coil conformation than a native tightly folded globular conformation). We have also recently observed that a partially folded intermediate of IgG light chains that form amyloid fibrils is relatively unfolded (16). Thus, it remains to be seen if it is a common feature in amyloid fibril formation that the critical monomeric partially folded intermediate is relatively unfolded.

The question arises as to the physiological significance of the observation of a partially folded intermediate of  $\alpha$ -synuclein formed under conditions of low pH or high temperature. Clearly, these particular environmental conditions will not be found in the dopaminergic cells of potential Parkinson's disease patients. However, the existence of such an intermediate, on the pathway to fibrils, means that *in vivo* conditions that lead to population of the intermediate will lead to increased risk of the disease. Thus, any intracellular factors that lead to a shift in the equilibrium position between the natively unfolded state and the partially folded intermediate will increase the likeli-

hood of  $\alpha$ -synuclein fibril formation. Such factors could include relatively nonpolar molecules that would preferentially bind to the intermediate, for example. Epidemiological studies have implicated insecticides and herbicides as increased risk factors for Parkinson's disease. In support of such a connection, we found in preliminary experiments<sup>2</sup> that several relatively hydrophobic pesticides as well as ANS both induce conformational changes in  $\alpha$ -synuclein and accelerate the rate of fibril formation, apparently by preferentially binding to the partially folded intermediate.

**Acknowledgments**—We thank Jon Krupp for help with the electron microscopy experiments and Ian Millet for assistance with the small angle x-ray scattering experiments.

#### REFERENCES

- Galvin, J. E., Lee, V. M., Schmidt, M. L., Tu, P. H., Iwatsubo, T., and Trojanowski, J. Q. (1999) *Adv. Neurol.* **80**, 313–324
- Okazaki, H., Lipkin, L. E., and Aronson, S. M. (1961) *J. Neuropathol. Exp. Neurol.* **21**, 422–449
- Trojanowski, J. Q., Goedert, M., Iwatsubo, T., and Lee, V. M. (1998) *Cell Death Differ.* **5**, 832–837
- Duffy, P. E., and Tennyson, V. M. (1965) *J. Neuropathol. Exp. Neurol.* **24**, 398–414
- Spillantini, M. G., Schmidt, M. L., Lee, V. M. Y., Trojanowski, J. Q., Jakes, R., and Goedert, M. (1997) *Nature* **388**, 839–840
- Spillantini, M. G., Crowther, R. A., Jakes, R., Hasegawa, M., and Goedert, M. (1998) *Proc. Natl. Acad. Sci. U. S. A.* **95**, 6469–6473
- Polymeropoulos, M. H., Lavedan, C., Leroy, E., Ide, S. E., Dehejia, A., Dutra, A., Pike, B., Root, H., Rubenstein, J., Boyer, R., Stenroos, E. S., Chandrasekharappa, S., Athanassiadou, A., Papapetropoulos, T., Johnson, W. G., Lazzarini, A. M., Duvoisin, R. C., Di Iorio, G., Golbe, L. I., and Nussbaum, R. L. (1997) *Science* **276**, 2045–2047
- Krüger, R., Kuhn, W., Müller, T., Woitalla, D., Graeber, M., Kösel, S., Przuntek, H., Eppelen, J. T., Schöls, L., and Riess, O. (1998) *Nat. Genet.* **18**, 106–108
- Arawaka, S., Saito, Y., Murayama, S., and Mori, H. (1998) *Neurology* **51**, 887–889
- Arima, K., Ueda, K., Sunohara, N., Hirai, S., Izumiyama, Y., Tonzuka-Uehara, H., and Kawai, M. (1998) *Brain Res.* **808**, 93–100
- Tu, P. H., Galvin, J. E., Baba, M., Giasson, B., Tomita, T., Leight, S., Nakajo, S., Iwatsubo, T., Trojanowski, J. Q., and Lee, V. M. (1998) *Ann. Neurol.* **44**, 415–422
- Kay, M. S., Ramos, C. H., and Baldwin, R. L. (1999) *Proc. Natl. Acad. Sci. U. S. A.* **96**, 2007–2012
- Maroteaux, L., Campanelli, J. T., and Scheller, R. H. (1988) *J. Neurosci.* **8**, 2804–2815
- Jakes, R., Spillantini, M. G., and Goedert, M. (1994) *FEBS Lett.* **345**, 27–32
- Weinreb, P. H., Zhen, W. G., Poon, A. W., Conway, K. A., and Lansbury, P. T., Jr. (1996) *Biochemistry* **35**, 13709–13715
- Khurana, R., Gillespie, J. R., Talapatra, A., Minert, L. J., Ionescu-Zanetti, C., Millet, I. S., and Fink, A. L. (2001) *Biochemistry* **39**, in press
- Goedert, M. (1997) *Nature* **388**, 232–233
- George, J. M., Jin, H., Woods, W. S., and Clayton, D. F. (1995) *Neuron* **15**, 361–372
- Iwai, A., Masliah, E., Yoshimoto, M., Ge, N., Flanagan, L., de Silva, H. A., Kittel, A., and Saitoh, T. (1995) *Neuron* **14**, 467–475
- Irizarry, M. C., Growdon, W., Gomezisla, T., Newell, K., George, J. M., Clayton, D. F., and Hyman, B. T. (1998) *J. Neuropathol. Exp. Neurol.* **57**, 334–337
- Davidson, W. S., Jonas, A., Clayton, D. F., and George, J. M. (1998) *J. Biol. Chem.* **273**, 9443–9449
- Jo, E., McLaurin, J., Yip, C. M., George-Hyslop, P., and Fraser, P. E. (2000) *J. Biol. Chem.* **275**, 34328–34334
- Jensen, P. H., Nielsen, M. S., Jakes, R., Dotti, C. G., and Goedert, M. (1998) *J. Biol. Chem.* **273**, 26292–26294
- Murphy, D. D., Rueter, S. M., Trojanowski, J. Q., and Lee, V. M. (2000) *J. Neurosci.* **20**, 3214–3220
- Crowther, R. A., Jakes, R., Spillantini, M. G., and Goedert, M. (1998) *FEBS Lett.* **436**, 309–312
- Wood, S. J., Wypych, J., Steavenson, S., Louis, J. C., Citron, M., and Biere, A. L. (1999) *J. Biol. Chem.* **274**, 19509–19512
- Serpell, L. C., Berriman, J., Jakes, R., Goedert, M., and Crowther, R. A. (2000) *Proc. Natl. Acad. Sci. U. S. A.* **97**, 4897–4902
- Uversky, V. N., Gillespie, J. R., and Fink, A. L. (2000) *Proteins Struct. Funct. Genet.* **41**, 415–427
- Naiki, H., Higuchi, K., Hosokawa, M., and Takeda, T. (1989) *Anal. Biochem.* **177**, 244–249
- Naiki, H., Higuchi, K., Matsushima, K., Shimada, A., Chen, W. H., Hosokawa, M., and Takeda, T. (1990) *Lab. Invest.* **62**, 768–773
- Oberg, K., Chrnyk, B. A., Wetzell, R., and Fink, A. L. (1994) *Biochemistry* **33**, 2628–2634
- Oberg, K. A., and Fink, A. L. (1998) *Anal. Biochem.* **256**, 92–106
- Wakatsuki, S., Hodgson, K. O., Eliezer, D., Rice, M., Hubbard, S., Gillis, N., and Doniach, S. (1992) *Rev. Sci. Instrum.* **63**, 1736–1740
- Tsuruta, H., Brennan, S., Rek, Z. U., Irving, T. C., Tompkins, W. H., and

<sup>2</sup> V. N. Uversky, J. Li, and A. L. Fink, unpublished data.

- Hodgson, K. O. (1998) *J. Appl. Crystallogr.* **31**, 672–682
35. Glatter, O., and Kratky, O. (1982) *Small Angle X-ray Scattering*, Academic Press Ltd., London
36. Creighton, T. E. (1993) in *Proteins: Structures and Molecular Properties* (Creighton, T. E., ed) W. H. Freeman & Co., New York
37. Baldwin, R. L. (1986) *Proc. Natl. Acad. Sci. U. S. A.* **83**, 8069–8072
38. Rodionova, N. A., Semisotnov, G. V., Kutysenko, V. P., Uverskii, V. N., and Bolotina, I. A. (1989) *Mol. Biol. (Mosc.)* **23**, 683–692
39. Semisotnov, G. V., Rodionova, N. A., Razgulyaev, O. I., Uversky, V. N., Gripas, A. F., and Gilmanshin, R. I. (1991) *Biopolymers* **31**, 119–128
40. Fink, A. L. (1999) in *The Encyclopedia of Molecular Biology* (Creighton, T. E., ed) pp. 140–142, John Wiley & Sons, Inc., New York
41. Gast, K., Damaschun, H., Eckert, K., Schulze-Forster, K., Maurer, H. R., Muller-Frohne, M., Zirwer, D., Czarnecki, J., and Damaschun, G. (1995) *Biochemistry* **34**, 13211–13218
42. Damaschun, G., Damaschun, H., Gast, K., Gernat, C., and Zirwer, D. (1991) *Biochim. Biophys. Acta* **1078**, 289–295
43. Uversky, V. N. (1993) *Biochemistry* **32**, 13288–13298
44. LeVine, H., II. (1995) *Neurobiol. Aging* **16**, 755–764
45. Bartl, F., Deckers-Hebestreit, G., Altendorf, K., and Zundel, G. (1995) *Biophys. J.* **68**, 104–110
46. Jarrett, J. T., and Lansbury, P. T. (1992) *Biochemistry* **31**, 12345–12352
47. Jarrett, J. T., and Lansbury, P. T., Jr. (1993) *Cell* **73**, 1055–1058
48. Lomakin, A., Teplow, D. B., Kirschner, D. A., and Benedek, G. B. (1997) *Proc. Natl. Acad. Sci. U. S. A.* **94**, 7942–7947
49. Schmid, F. X. (1995) *Curr. Biol.* **5**, 993–994
50. Buchet, R., Varga, S., Seidler, N. W., Molnar, E., and Martonosi, A. (1991) *Biochim. Biophys. Acta* **1068**, 201–216
51. Fahmy, K., Jager, F., Beck, M., Zvyaga, T. A., Sakamar, T. P., and Siebert, F. (1993) *Proc. Natl. Acad. Sci. U. S. A.* **90**, 10206–10210